

Electronic Supplementary Information (ESI)

for

Achieving Efficient Organic Solar Cells via Synergistically Doping Active Layer and Interface by A Conjugated Macrocycle

*Yan Wang, Yi Zhang, Tong Shan, Qingyun Wei, Zhenchuang Xu, Yanchuan Zhao, Jianming Yang, Qinye Bao, Hui Jin, Zaifei Ma, Hao Wei, and Hongliang Zhong**

1. Experimental Section

Notation and meaning

In this article and ESI, we use several special notations for simplification as followed:

Notations	Detailed Illustration
CS	Cyanostar
PM6+CS	PM6 and cyanostar are directly mixed together
Y6+CS	Y6 and cyanostar are directly mixed together
PM6+Y6	PM6 and Y6 are directly mixed together
PM6/Y6	Sequential deposition followed by PM6 and Y6 order
CS/PM6/Y6	Sequential deposition followed by cyanostar, PM6, and Y6 order
PM6+CS/Y6	Sequential deposition followed by PM6+CS and Y6 order
PM6/Y6+CS	Sequential deposition followed by PM6 and Y6+CS order
PM6:Y6:CS	Blend coating of PM6, Y6, and cyanostar to fabricate an OSC device
CS/PM6:Y6	Blend coating of PM6 and Y6 after cyanostar layer to fabricate an OSC device

Materials

The PM6 was purchased from Organtec Ltd. The Y6 was purchased from Vizhchem technology Co. Ltd. The PDINO was purchased from J&K Scientific Co. Ltd. Anhydrous solvents were commercially available without further purification.

Characterization Methods

The UV-vis absorption spectra were measured by Lambda 750S spectrophotometer with dilute solutions and films. The atomic force microscopy (AFM) was measured by a Bruker Multimode 8 via tapping mode under atmosphere conditions at room temperature. The Grazing-incidence wide-angle X-ray scattering (GIWAXS) characterization of the thin films was performed at the BL14B1 beamline of Shanghai Synchrotron Radiation Facility (SSRF) on beamline 14. Samples were prepared under device conditions on the Si/PEDOT:PSS substrates. The X-ray beam (10 keV) was incident at a grazing angle of 0.16° . The spectra of time-of-flight-secondary ion mass spectrometry (TOF-SIMS) were obtained by a GAIA3 GMU model 2016 scanning electron microscope. The steady state PL spectra were measured on a FLS1000 photoluminescence spectrometer with an excitation wavelength of 560 nm for PM6 and 660 nm for Y6.

Device Characterization

The device $J-V$ characteristics were tested by a Keithley 2420 SourceMeter unit in forward direction under AM 1.5 G (1.0 Sun) irradiance (100 mW cm^{-2}) as generated by a 300 W Xe lamp solar simulator (Enlitech SS-F5-3A) at room temperature. The light intensity was calibrated using a standard Si diode with KG-5 filter. The EQE spectra were characterized *via* an Enlitech EQE system (Enlitech QE-M110) with a Si diode as reference cell. Monochromatic light was generated from an Enlitech lamp source with a monochromator.

The transient photovoltage decay measurements were done using two white LED lamps, driven by a Keithley 2450 source meter for different bias illumination intensities and an arbitrary function generator (AFG3022C, Tektronix) for the transient illumination. The peaks of the transient voltage signals, recorded by an oscilloscope (MDO4104C, Tektronix), were kept to approximated 5% of the DC bias photovoltage signal, by adjusting the driving voltage of the LED controlled by the function generator for each bias illumination intensity,

and the record transient photovoltage decay signals were fitted using an exponential decay function.

Charge Carrier Mobility Measurement

Hole-only diode configuration: ITO/PEDOT:PSS/active layers/MoO₃/Ag. Electron-only diode configuration: ITO/ZnO/active layers/PDINO/Ag. PEDOT:PSS, MoO₃, PDINO, and Ag were deposited by the same route as OSC devices. The mobility in active layers were determined by fitting the dark current hole/electron-only diodes to the space-charge limited current (SCLC) model. The mobility was determined by the equation 1:

$$J = \frac{9\varepsilon_0\varepsilon_r\mu_0V^2}{8d^3} \quad 1$$

where J is current density, μ_0 is the hole or electron mobility, ε_r is the dielectric permittivity of the active layer (generally assumed to be 3 for organic materials), ε_0 is the dielectric permittivity of free space ($\varepsilon_0 = 8.854187817 \times 10^{-12}$ F m⁻¹), d is the film thickness of active layers, and V is the voltage, which is defined as $V = V_{\text{appl}} - V_{\text{bi}}$, where V_{appl} is the applied voltage, V_{bi} is the built-in voltage.

2. OSCs Fabrication

The solar cell devices were fabricated in the conventional configuration: indium tin oxide (ITO)/poly(3,4-ethylene dioxythiophene):polystyrene sulfonate (PEDOT:PSS)/active layer/PDINO/Ag. The patterned indium tin oxide glass (ITO) glass substrates (sheet resistance = 10 Ω sq⁻¹) were cleaned in detergent, de-ion water, acetone, chloroform, acetone, and isopropanol sequentially by ultra-sonic bath for 15 min each and then dried by N₂ gas. Further UV-Ozone treatment for 10 min was applied before using. The PEDOT:PSS solution was spin-coated onto the cleaned ITO glass substrate at 3000 rpm of 35 s followed by annealing at 150 °C of 15 min in the air to obtain 35 nm film approximately. Then the PEDOT:PSS coated substrates were transferred into a nitrogen-filled glove box. The PM6 with/without 3 wt% cyanostar was dissolved in chlorobenzene (CB, the concentration of PM6 solution was 9 mg mL⁻¹) and stirred at 60 °C for 5 hours in a nitrogen-filled glove box to form PM6 or PM6+CS solution. The Y6 with/without 3 wt% CS were dissolved in chloroform (CF, the concentration of Y6 solution was 9 mg mL⁻¹) with the solvent additive of 1-chloronaphthalene (CN, 0.5 % vol), and stirred at 45 °C for 1 hour in the nitrogen-filled glove box to form Y6 or Y6+CS solution. The CS solution was dissolved in CF (the concentration of CS solution was 3 mg mL⁻¹), and stirred at room temperature for 30 min in the nitrogen-filled glove box. Then the CS solution was spin-coated onto the PEDOT:PSS substrate for CS/PM6/Y6 device. PM6 or PM6+CS solution was then spun followed by Y6 or Y6+CS solution to form a 120 nm-thick layer in total. The spun-cast devices were baked on a hot plate at various temperatures for 5 min at 90°C. Then, a 1 mg mL⁻¹ PDINO dissolved in methanol was spin-coated onto the active layer at 3000 rpm for 30 s to form a ~10 nm-thick electron transport layer. Finally, the anode, 100 nm Ag was deposited at a speed of 0.3 nm/s through a shadow mask by thermal evaporation in a vacuum chamber of under 2×10^{-4} Pa to complete the device fabrication. The active area of each device was defined to 3.64 mm².

The inverted devices were fabricated in the configuration: ITO/ZnO/PFN-Br/active layer/MoO₃/Ag. The patterned ITO glass substrates were treated as previously mentioned. The ZnO nanoparticles were spin-coated onto the cleaned ITO glass substrate at 3000 rpm of 30 s, followed by the deposition a thin layer of PFN-Br. The PM6/Y6 blend solutions with/without cyanostar were spin-coated as the active layer with the thickness around 110 nm. Then, 10 nm MoO₃ was deposited at a speed of 0.06 nm/s followed by 100 nm Ag by thermal evaporation in a

vacuum chamber of under 2×10^{-4} Pa to complete the device fabrication. The active area of each device was defined to 3.64 mm².

2. Supplementary Figures

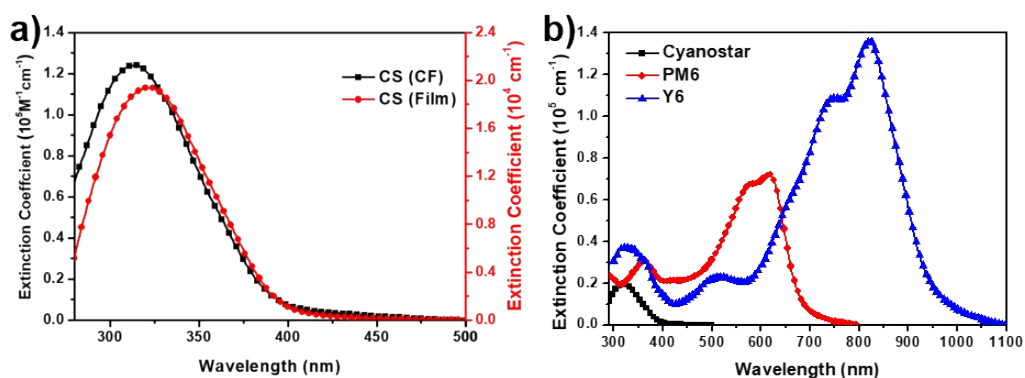


Fig. S1 Extinction coefficient of a) cyanostar (CS) in chloroform (CF) and solid state, b) cyanostar, PM6, and Y6 in solid state, respectively.

Absorption o

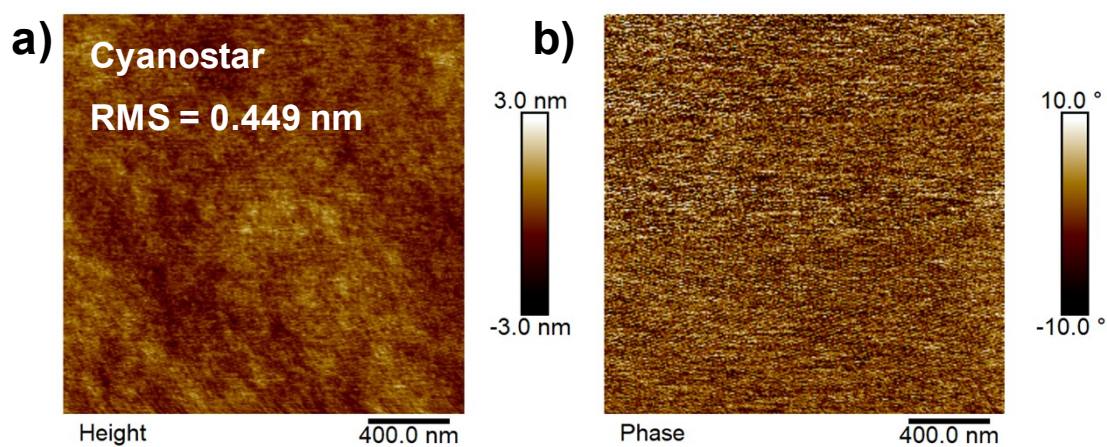


Fig. S2 AFM height (a) and phase (b) images of cyanostar neat film, respectively

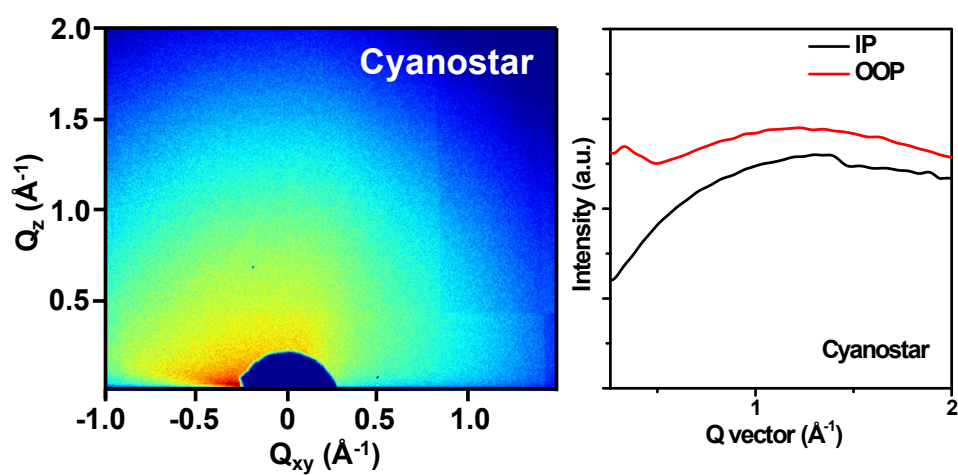


Fig. S3 (a) 2D GIWAXS diffraction patterns and (b) corresponding 1D cutline profiles of cyanostar neat film, respectively.

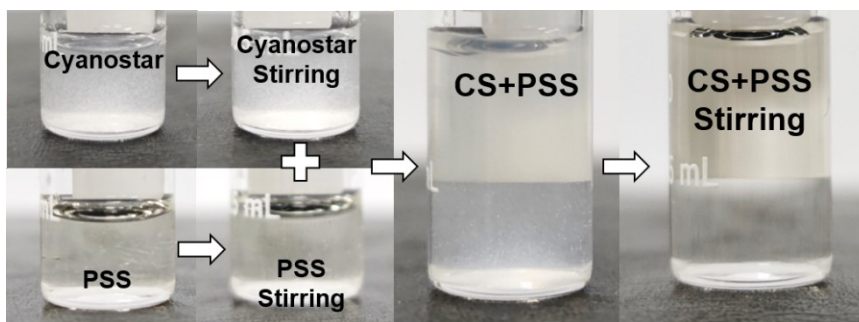


Fig. S4 Photo images of cyanostar, PSS in isopropanol (IPA) with or without stirring. The CS+PSS sample was mixed with the cyanostar stirring and PSS stirring samples.

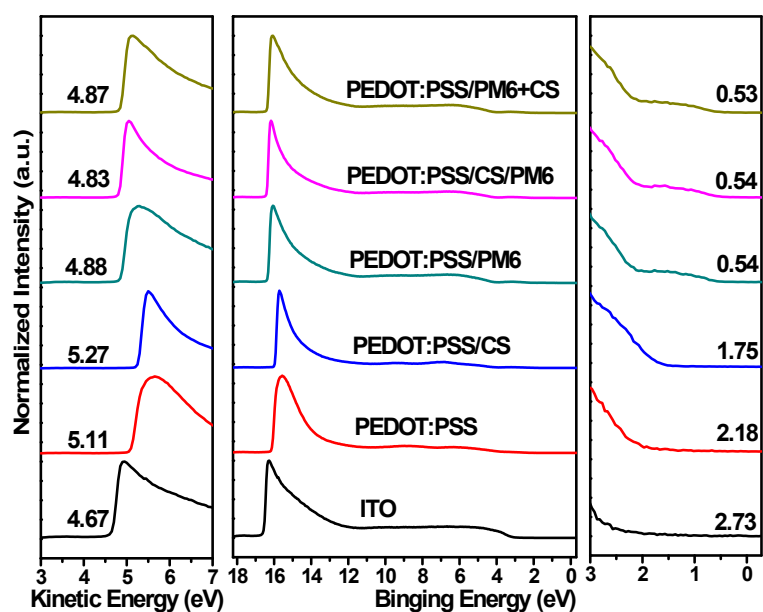


Fig. S5 UPS spectra of PM6, CS/PM6, PM6+CS, and PM6/CS with PEDOT:PSS substrate, respectively.

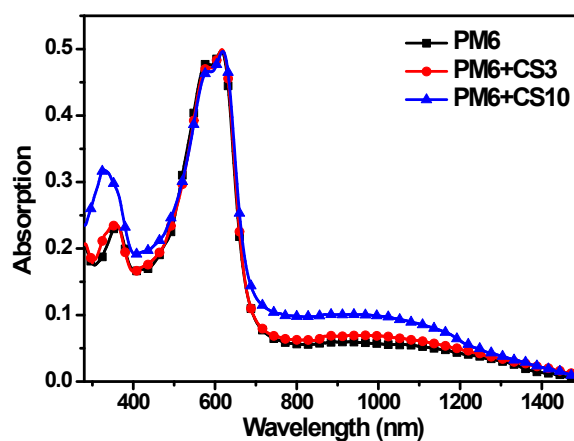


Fig. S6 Absorption in solid state of PM6, PM6+CS3, and PM6+CS10, respectively.

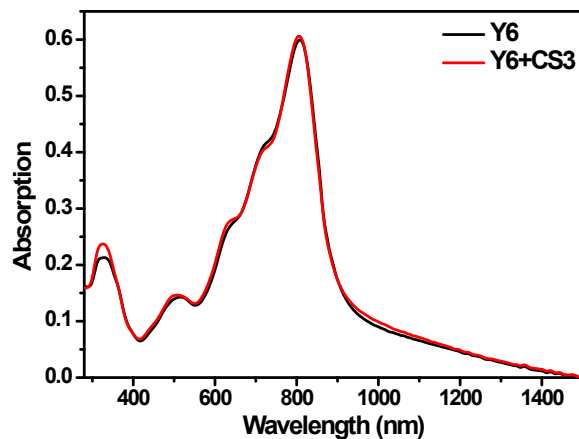


Fig. S7 Absorption in solid state of Y6 and Y6+CS3, respectively.

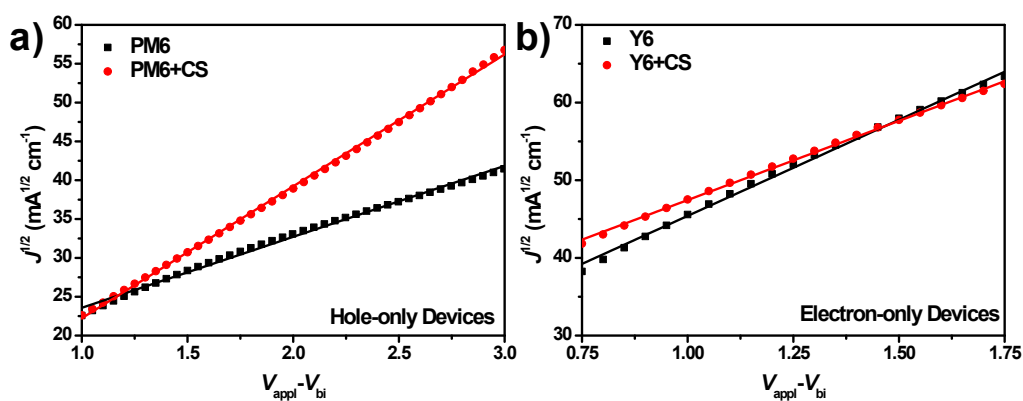


Fig. S8 Plots of $J^{1/2}$ as a function of $V_{app1} - V_{bi}$ for the (a) hole-only devices of PM6 and PM6+CS and (b) electron-only devices of Y6 and Y6+CS, respectively.

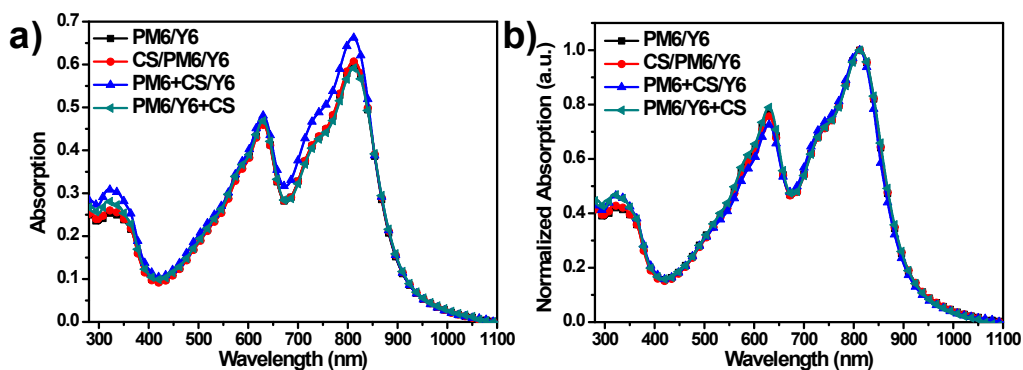


Fig. S9 (a) Absorption and (b) Normalized absorption of optimized PM6/Y6, CS/PM6/Y6, PM6+CS/Y6, and PM6/Y6+CS blend films, respectively.

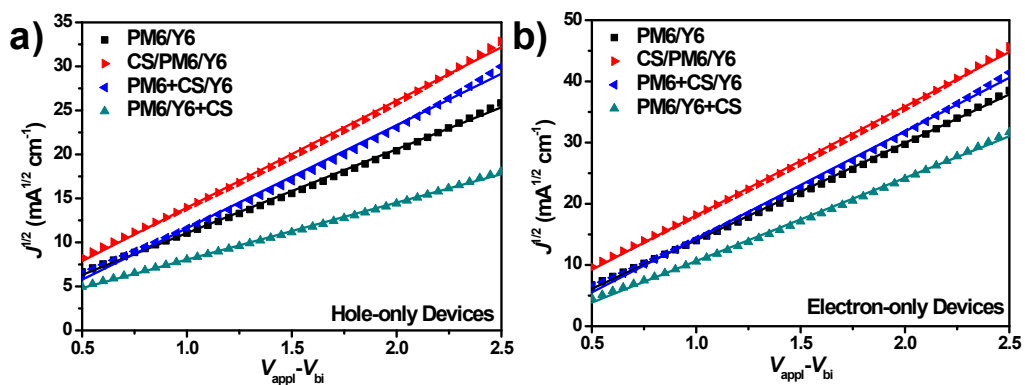


Fig. S10 Plots of $J^{1/2}$ as a function of $V_{\text{appl}} - V_{\text{bi}}$ for the (a) hole-only devices and (b) electron-only devices of PM6/Y6, CS/PM6/Y6, PM6+CS/Y6, and PM6/Y6+CS based devices, respectively.

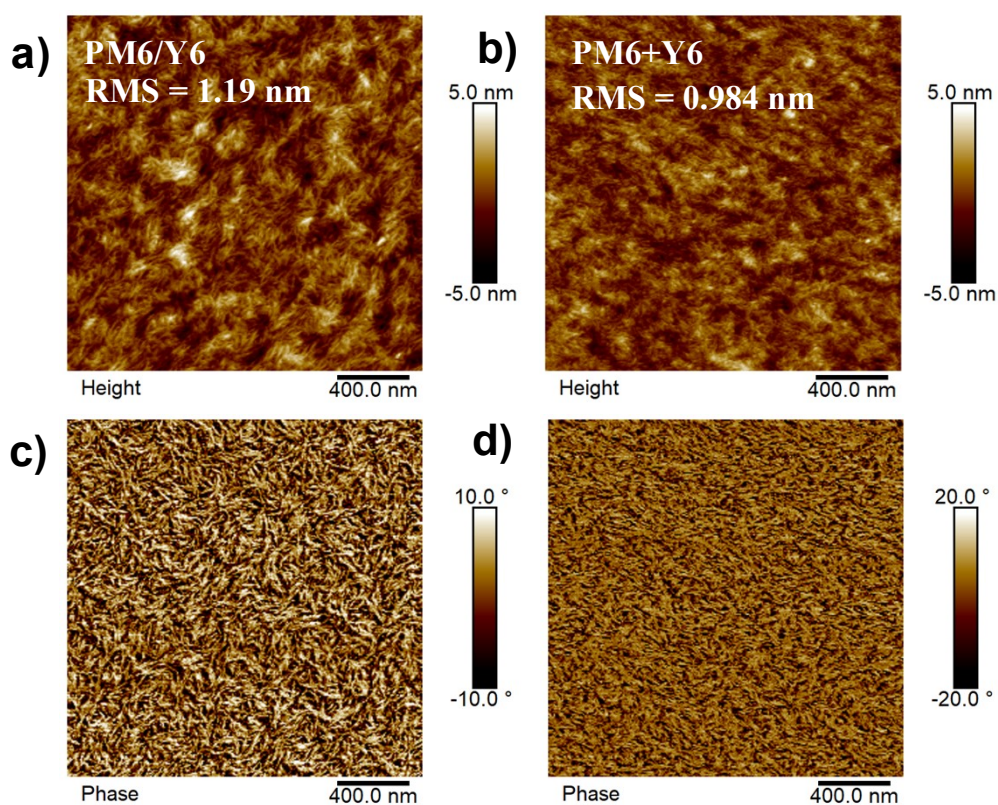


Fig. S11 AFM height (a and b) and phase (c and d) images of PM6/Y6 and PM6+Y6 blend films, respectively.

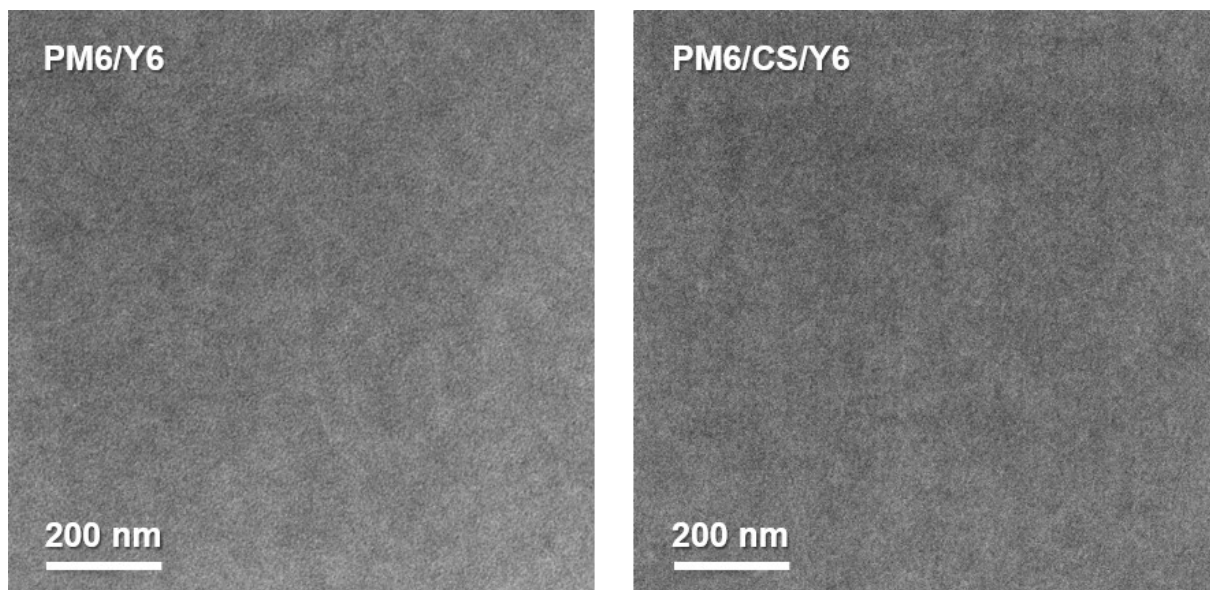


Fig. S12 TEM images of PM6/Y6 (left) and CS/PM6/Y6 (right) blend films.

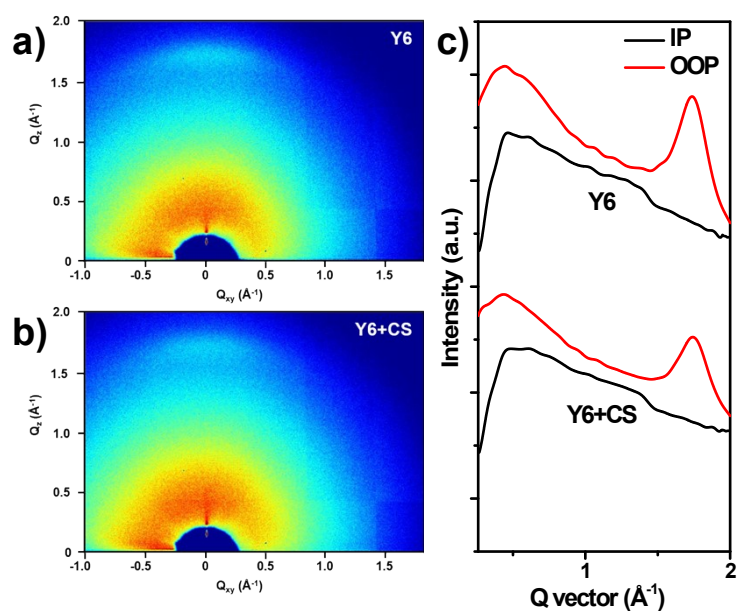


Fig. S13 2D GIWAXS diffraction patterns (a and b) and corresponding 1D cutline profiles (c) of Y6 neat film and Y6+CS blend film, respectively.

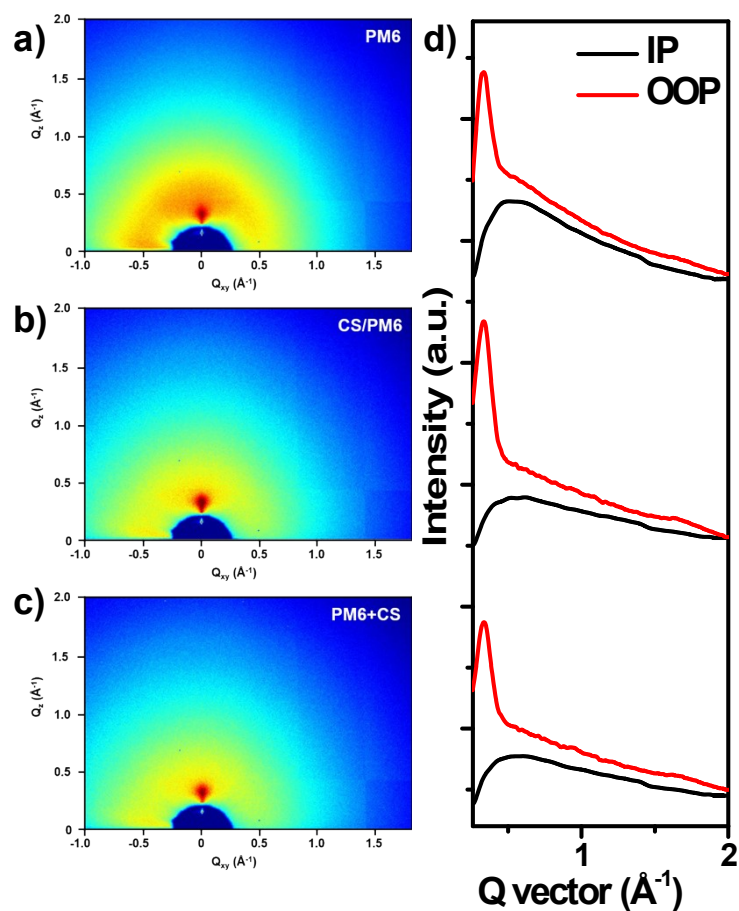


Fig. S14 (a), (b), and (c) 2D GIWAXS diffraction patterns and d) corresponding 1D cutline profiles of PM6 neat film and CS/PM6 and PM6+CS blend films, respectively.

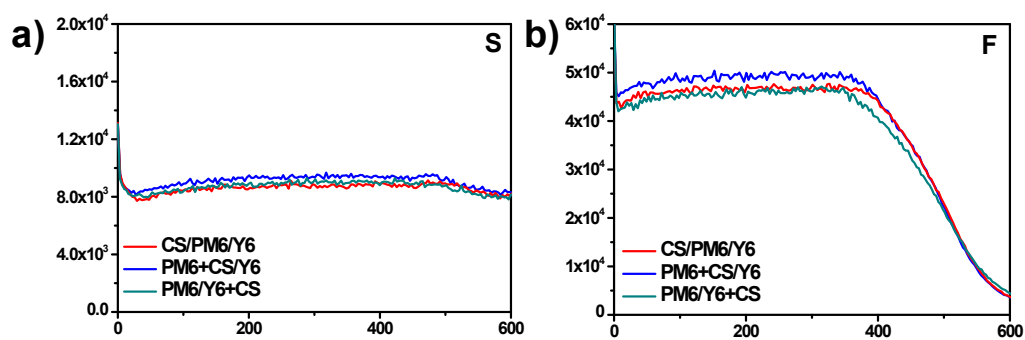


Fig. S15 (a) The S and (b) F signal from TOF-SIMS of CS/PM6/Y6, PM6+CS/Y6, and PM6/Y6+CS blend films, respectively.

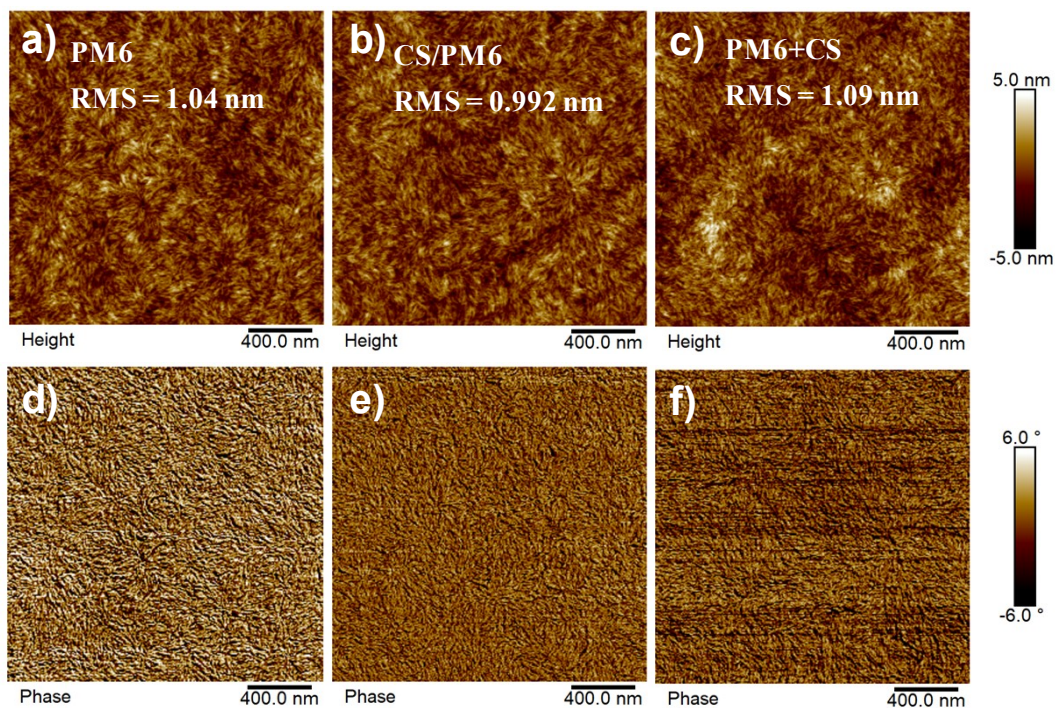


Fig. S16 AFM height (a, b, and c) and phase (d, e, and f) images of PM6 neat film, CS/PM6, and PM6+CS blend films, respectively.

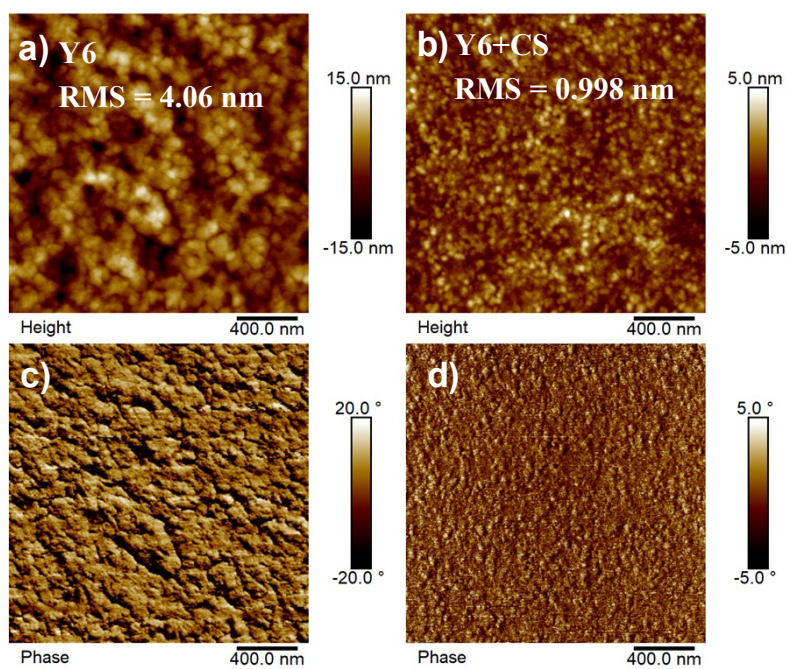


Fig. S17 AFM height (a and b) and phase (c and d) images of Y6 neat film and Y6+CS blend film, respectively.

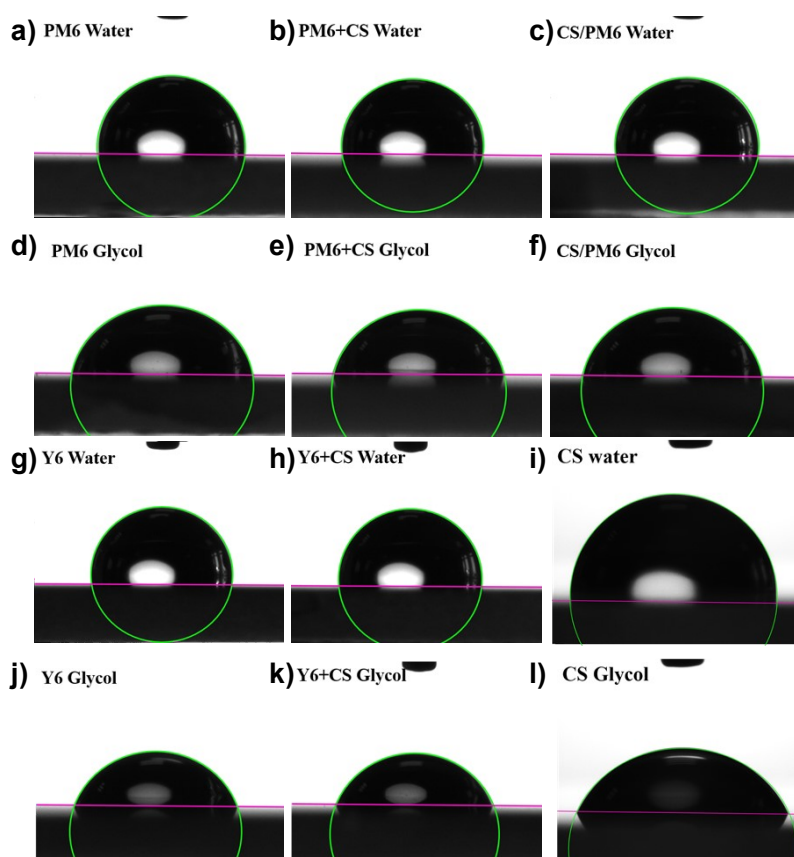


Fig. S18 Contact angle of water and glycol phase based on PM6 (a and d), PM6+CS (b and e), CS/PM6(c and f), Y6 (g and j), Y6+CS (h and k), and CS (i and l), respectively.

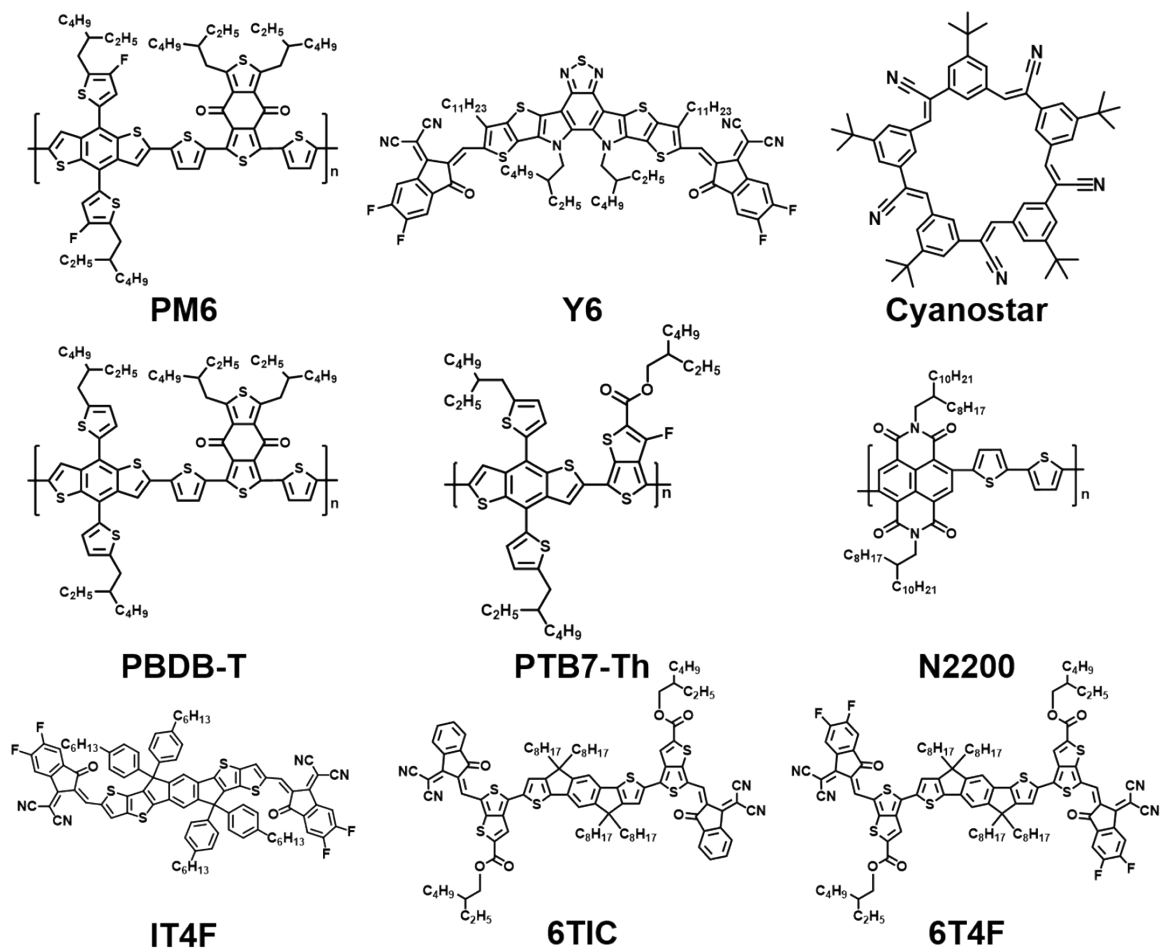


Fig. S19 Chemical structures of the donors and acceptors applied in the article and supporting information, respectively.

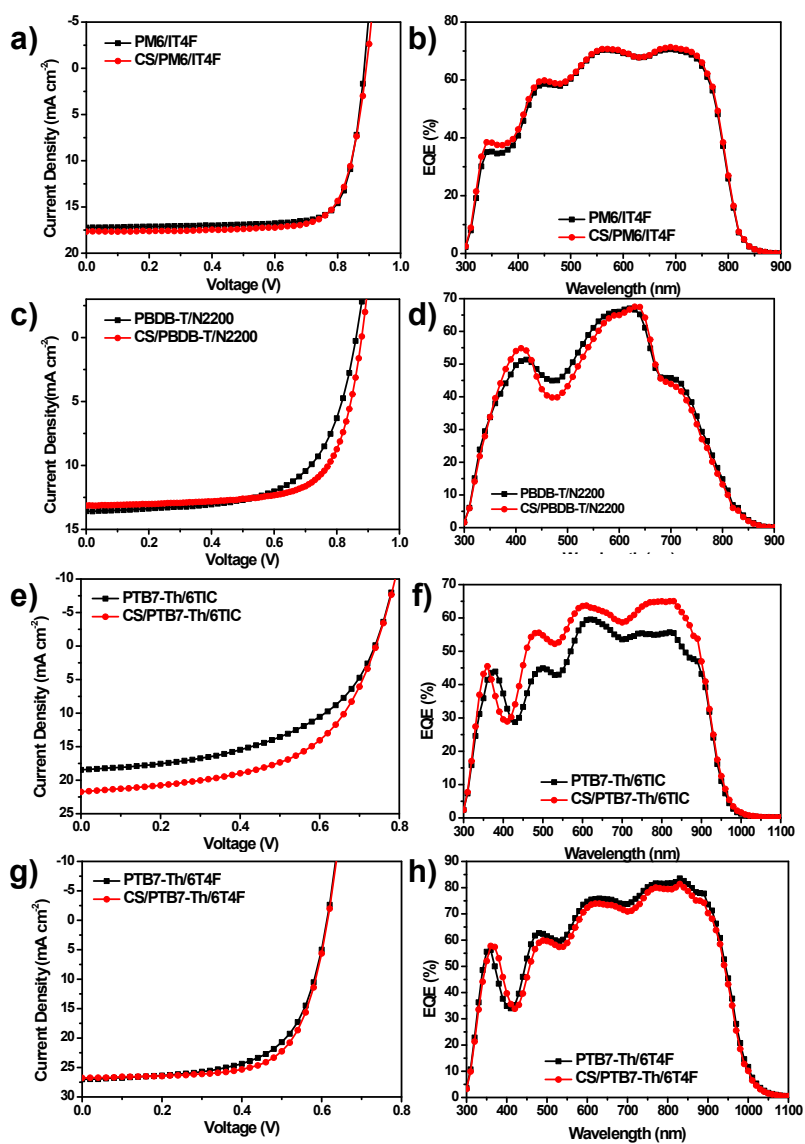


Fig.S20 *J-V* (a, c, e, and g) and EQE (b, d, f, and h) curves of optimized pseudo-bilayer OSCs with/without CS, respectively.

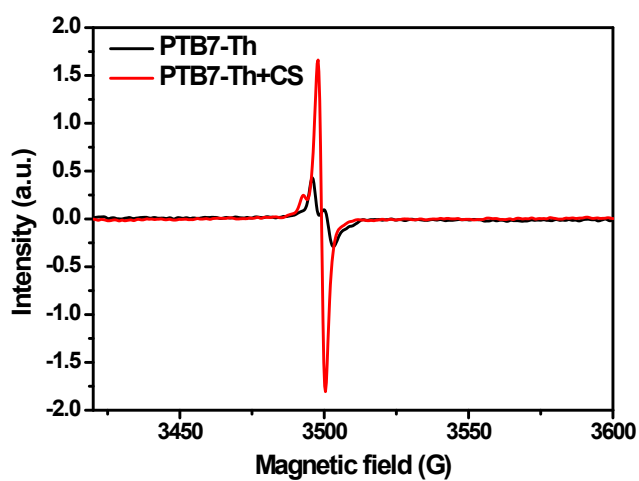


Fig. S21 ESR spectra of PTB7-Th and PTB7-Th+CS in film state, respectively.

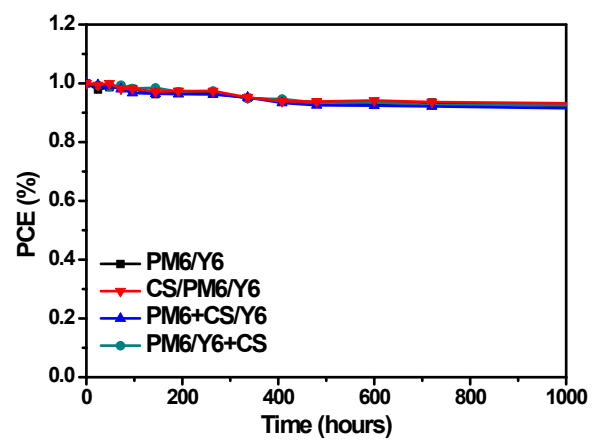


Fig. S22 The degradation curves of PCEs when the devices are stored in nitrogen-filled glove box.

3. Supplementary Tables

Table S1. Hole mobility of PM6, PM6+CS, and CS/PM6, and electron mobility of Y6, Y6+CS and CS/Y6 based devices, respectively.

Donor	μ_h (cm ² V ⁻¹ s ⁻¹)	Acceptor	μ_e (cm ² V ⁻¹ s ⁻¹)
PM6	4.65×10 ⁻⁵	Y6	2.27×10 ⁻⁴
PM6+CS	1.61×10 ⁻⁴	Y6+CS	1.54×10 ⁻⁴
CS/PM6	2.41×10 ⁻⁴	CS/Y6	2.35×10 ⁻⁴

Table S2. The detailed optimization parameters of the control devices of ITO/PEDOT:PSS/PM6/Y6/PDINO/Ag *via* sequential deposition.

Optimization	PM6 Layer	Y6 Layer	V_{oc} (V)	J_{sc} (mA cm ⁻²)	FF (%)	PCE (%)
Spin Speed	1600 rpm		0.842	25.31	77.2	16.45
	1900 rpm	2450 rpm	0.845	25.27	77.7	16.59
	2200 rpm		0.847	24.81	78.4	16.48
		2250 rpm	0.843	25.69	76.0	16.36
	1900 rpm	2650 rpm	0.847	25.04	77.7	16.49

Table S3. The detailed optimization parameters of the CS based devices with different pseudo-bilayer configuration *via* sequential deposition.

Different Devices	CS content	V_{oc} (V)	J_{sc} (mA cm ⁻²)	FF (%)	PCE (%)
PM6+CS/Y6	5 wt%	0.852	25.74	77.5	17.01
	3 wt%	0.856	26.09	78.0	17.43
	1 wt%	0.858	25.74	78.1	17.25
PM6/Y6+CS	5 wt%	0.860	24.12	76.1	15.79
	3 wt%	0.859	24.33	77.2	16.14
	1 wt%	0.854	24.46	76.7	16.03
CS (in CF) /PM6/Y6	5 mg mL ⁻¹ (136 nm)	0.855	26.28	78.8	17.72
	3 mg mL ⁻¹ (85 nm)	0.854	26.71	78.8	17.98
	1 mg mL ⁻¹ (28 nm)	0.853	26.41	78.6	17.71

Table S4. The contact angle and surface energy of PM6, PM6+CS, CS/PM6, PM6/CS, Y6, Y6+CS, CS/Y6, Y6/CS and CS, respectively.

	Water [°] ^a	Glycol [°] ^a	γ [mN m ⁻¹]
PM6	99.2	80.1	30.02
PM6+CS	101.3	78.9	29.11
CS/PM6	99.8	77.5	27.62
PM6/CS	99.1	77.7	37.12
Y6	99.8	71.5	36.78
Y6+CS	101.3	71.5	41.64
CS/Y6	94.3	71.5	33.53
Y6/CS	86.6	69.7	50.93
CS	89.4	65.6	37.21

^a The average values are statistical data from five independent measurements.

Table S5. The interaction parameter of PM6, PM6+CS, CS/PM6, PM6/CS, Y6, Y6+CS, CS/Y6 and Y6/CS, respectively.

χ	Y6	Y6+CS	CS
PM6	0.343	0.948	0.386
PM6+CS	0.448		
CS/PM6	0.655		
CS	0.001		

Table S6. Photovoltaic performances of conventional OSCs with/without CS, respectively. The device configuration is ITO/PEDOT:PSS/active layer/PDINO/Ag *via* blend coating.

Active Layer	V_{oc} [V]	J_{sc} [mA cm ⁻²]	FF [%]	PCE [%]
PM6:Y6	0.85	25.22	71.0	15.23
PM6:Y6:CS	0.86	24.91	72.4	15.50

Table S7. Photovoltaic performances of inverted OSCs with/without CS, respectively. The device configuration is ITO/ZnO/PFN-Br/active layer/MoO₃/Ag *via* blend coating.

Active Layer	V_{oc} [V]	J_{sc} [mA cm ⁻²]	FF [%]	PCE [%]
PM6:Y6	0.84	24.05	72.6	14.67
PM6:Y6:CS	0.84	24.78	73.1	15.21

Table S8. Photovoltaic performances of optimized OSCs with/without CS, respectively. The device configuration is ITO/PEDOT:PSS/(CS)/active layer/PDINO/Ag *via* sequential deposition.

Active Layer	V_{oc} [V] ^a	J_{sc} [mA cm ⁻²] ^a	J_{cal} [mA cm ⁻²] ^b	FF [%] ^a	PCE [%] ^a
PM6/IT4F	0.884±0.003	17.09±0.02	17.26	78.7±0.5	11.89±0.14 (12.04)
CS/PM6/IT4F	0.891±0.002	17.58±0.21	17.48	76.8±0.1	12.03±0.15 (12.22)
PBDB-T/N2200	0.861±0.004	13.57±0.02	13.68	63.3±0.5	7.40±0.02 (7.42)
CS/PBDB-T/N2200	0.877±0.03	13.06±0.07	13.24	70.0±0.3	8.02±0.12 (8.15)
PTB7-Th/6TIC	0.740±0.002	18.10±0.19	17.53	50.1±0.3	6.71±0.08 (6.79)
CS/PTB7-Th/6TIC	0.743±0.002	21.35±0.28	20.03	55.4±0.2	8.79±0.05 (8.83)
PTB7-Th/6T4F	0.612±0.003	26.99±0.08	25.63	63.3±0.5	10.45±0.04(10.48)
CS/PTB7-Th/6T4F	0.614±0.002	26.89±0.18	24.70	68.0±0.1	11.20±0.02 (11.22)

^a The average values and standard deviations are statistical data from ten independent cells. The values in parentheses are the champion efficiency of the optimized OSCs; ^b The integral J_{sc} is calculated from the EQE curves.